Thin-Walled Structures 106 (2016) 258–267

Contents lists available at ScienceDirect

Thin-Walled Structures

journal homepage: www.elsevier.com/locate/tws

On the nonlinear stability of eccentrically stiffened functionally graded annular spherical segment shells

Dinh Duc Nguyen*, Huy Bich Dao, Thi Thuy Anh Vu

Vietnam National University, Hanoi, 144 Xuan Thuy, Cau Giay, Hanoi, Vietnam

ARTICLE INFO

Article history:
Received 11 March 2016
Received in revised form
11 May 2016
Accepted 11 May 2016

Keywords:
Nonlinear stability
Eccentrically stiffened FGM annular spherical segment shells
Elastic foundations
External pressure

ABSTRACT

The nonlinear stability of eccentrically stiffened functionally graded (FGM) annular spherical segment resting on elastic foundations under external pressure is studied analytically. The FGM annular spherical segment are reinforced by eccentrically longitudinal and transversal stiffeners made of full metal or ceramic depending on situation of stiffeners at metal-rich or ceramic-rich side of the shell respectively. Based on the classical thin shell theory, the governing equations of FGM annular spherical segments are derived. Approximate solutions are assumed to satisfy the simply supported boundary condition of segments and Galerkin method is applied to study the stability. The effects of material, geometrical properties, elastic foundations, combination of external pressure and stiffener arrangement, number of stiffeners on the nonlinear stability of eccentrically stiffened FGM annular spherical segment are analyzed and discussed. The obtained results are verified with the known results in the literature.

1. Introduction

In recent years, many authors have focused on the static and dynamic of eccentrically stiffened plate and shell structures because these structures usually reinforced by stiffening members to provide the benefit of added load-carrying static and dynamic capability with a relatively small additional weight penalty. In additions, eccentrically stiffened plate and shell is a very important structure in engineering design of aircraft, missile and aerospace industries. As a result, there are many researches on the static and dynamic of eccentrically stiffened shell and plate structures, especially structures made of composite material.

For the eccentrically stiffened plate, the elastic stability of eccentrically stiffened plates [1] was studied by Meiwen and Issam by a finite element model. The formulation was based on the behavior of the plate-stiffener system and accounts for the different neutral surfaces for bending in the x-z and y-z planes. Duc and Cong [2] studied the nonlinear post-buckling of an eccentrically stiffened thin FGM plate resting on elastic foundations in thermal environments by using a simple power-law distribution. An experimental study on stiffened plates subjected to combined action of in-plane load and lateral pressure is described in [3] by Shanmugam et al. The paper [4] presented a periodic concept in stiffened-thin-plates by applying Bloch's theorem. Through the established dynamic equation for periodically stiffened-thin-plate (PSTP), the band gap of PSTP is calculated with the help of center-finite-difference-method (CFDM) by Zhou et al.

Studies on the static and dynamics were carried out with eccentrically stiffened shallow shells made of laminated composite material. For example, Li and Qiao [5] studied the nonlinear free vibration and parametric resonance analysis for a geodesically-stiffened anisotropic laminated thin cylindrical shell of finite length subjected to static or periodic axial forces using the boundary layer theory. In [6], by Sarmila, the finite element method has been applied to analyze free vibration problems of laminated composite stiffened shallow spherical shell panels with cutouts employing the eight-noded curved quadratic iso-parametric element for shell with a three noded beam element for stiffener formulation. For the composite stiffened laminated cylindrical shells, in [7], by Li et al., a layerwise theory was used to model the behavior of the composite laminated cylindrical shells, and the eight-noded solid element is employed to discrete the stiffeners, and then, based on the governing equations of the shells and stiffeners, governing equation of the composite stiffened laminated cylindrical shells was assembled by using the compatibility conditions to ensure the compatibility of displacements at the interface between shells and stiffeners. Li and Yang [8] investigated the post-buckling of shear deformable stiffened an isotropic laminated cylindrical shell under axial compression. Formulation of the dynamic stiffness of a crossply laminated circular cylindrical shell subjected to distributed loads was studied by Casimir et al. [9]. By using the commercial ANSYS finite element software, Less and Abramovich [10] studied the dynamic buckling of a laminated composite stringer stiffened cylindrical panel. Bich

* Corresponding author.
E-mail address: ducnd@vnu.edu.vn (D.D. Nguyen).

http://dx.doi.org/10.1016/j.tws.2016.05.006
0263-8231/

Nomenclature

k	The volume fraction index (non-negative number)
w	The deflection of the annular spherical shell
k_1	The Winkler foundation modulus
k_2	The shear layer foundation stiffness of Pasternak model.
$\varepsilon_r^0,\ \varepsilon_\theta^0$	The normal strains
$\gamma_{r\theta}^0$	The shear strain at the middle surface of the spherical shell
$\chi_r, \chi_\theta, \chi_{r\theta}$	The changes of curvatures and twist
s_1, s_2	The distance between eccentrically longitudinal and latitude stiffeners respectively
A_1, A_2	The cross-sectional area of eccentrically longitudinal and latitude stiffeners respectively
$d_1,\ d_2,\ h_1,\ h_2$	The width and height of eccentrically longitudinal and latitude stiffeners respectively
$n_1,\ n_2$	The numbers of eccentrically longitudinal and latitude stiffeners respectively
E_0	The Young's modulus of the stiffeners. $E_0 = E_c$ if the stiffeners are reinforced at the surface of the ceramic-rich, $E_0 = E_m$ if the stiffeners are reinforced at the surface of the metal-rich

et al. [11] presented analytical approach to investigate the nonlinear dynamic of imperfect reinforced laminated composite plates and shallow shells using the classical thin shell theory with the geometrical nonlinearity in von Karman–Donnell sense and the smeared stiffeners technique.

As well as know a functionally graded material (FGM) is a two-component composite characterized by a compositional gradient from one component to the other. In contrast, traditional composites are homogeneous mixtures, and they therefore involve a compromise between the desirable properties of the component materials. Since significant proportions of an FGM contain the pure form of each component, the need for compromise is eliminated. The properties of both components can be fully utilised. This is mainly due to the increasing use of FGM as components of structures in the advanced engineering. For FGM, many researches focused on the static and dynamical analysis of stiffened shallow shells. For example, recently, Duc et al. [12–19] has published several studies on the eccentrically stiffened shell structures made of FGM and the majority of these studies have been synthesized in the book [28]. First example [12] Duc studied the nonlinear thermal dynamic analysis of eccentrically stiffened S-FGM circular cylindrical shells surrounded on elastic foundations using the Reddy's third-order shear deformation shell theory [13], presented nonlinear mechanical, thermal and thermo-mechanical post-buckling of imperfect eccentrically stiffened thin FGM cylindrical panels on elastic foundations [14], investigated nonlinear dynamic response of imperfect eccentrically stiffened doubly curved FGM shallow shells on elastic foundations [15], presented nonlinear post-buckling of imperfect eccentrically stiffened FGM double curved thin shallow shells in thermal environments [16], studied nonlinear response of imperfect eccentrically stiffened ceramic-metal-ceramic S-FGM circular cylindrical shells surrounded on elastic foundations and subjected to axial compression. Bich et al. studied nonlinear post-buckling and dynamic of eccentrically stiffened functionally graded shallow shells and panels [20,21], besides a lot of other researchers by the same authors. In addition, linear static buckling of FGM axially loaded cylindrical shell reinforced by ring and stringer FGM stiffeners has studied by Najafizadeh et al. [22]. Accurate buckling solutions of grid-stiffened functionally graded cylindrical shells under compressive and thermal loads has studied by Sun et al. [23].

The annular spherical shell and annular spherical segment are two of the special shapes of the spherical shells. An annular spherical segment or an open annular spherical shell limited by two meridians and two parallels of a spherical shell. It has become popularly in engineering designs, but despite the evident importance in practical applications, from the open literature that investigations on the thermo-elastic, dynamic and buckling analysis of annular spherical segment is comparatively scarce. In addition, the special geometrical shape of this structure is a big difficulty to find the explicit solution form. Can enumerate some studies of annular spherical shell and segment as Bich and Phuong [24] investigated the buckling analysis of FGM annular spherical shells and segments subjected to compressive load and radial pressure. Most recently, Anh et al. analyzed the nonlinear buckling analysis of thin FGM annular spherical shells on elastic foundations under external pressure and thermal loads in [25], the nonlinear stability of axisymmetric FGM annular spherical shells under thermo-mechanical load in [26,27] investigated the nonlinear stability of thin FGM annular spherical segment resting on elastic foundations in thermal environment.

In this paper, the nonlinear analysis of eccentrically stiffened FGM annular spherical segment shells is investigated. The segment-shells are reinforced by eccentrically longitudinal and transversal stiffeners made of full metal or full ceramic depending on situation of stiffeners at metal-rich side or ceramic-rich side of the shell respectively. The paper analyzed and discussed the effects of material and geometrical properties, elastic foundations and eccentrically stiffeners on the stability of the eccentrically stiffened FGM annular spherical segment.

2. Functionally graded annular spherical shell and elastic foundation

Consider a FGM annular spherical segment or a FGM open annular spherical shell limited by two meridians and two parallels of a spherical shell resting on elastic foundations with radius of curvature R, base radii of lower and upper bases r_1, r_0 respectively, open angle of two meridional planes β and thickness h. The FGM annular spherical segment reinforced by eccentrically longitudinal and transverse stiffeners is subjected to external pressure q uniformly distributed on the outer surface as shown in Fig. 1.

Assume that the FGM segment – shell is made from a mixture of ceramic and metal constituents and the effective material properties vary continuously along the thickness by the power law distribution

$$V_c(z) = \left(\frac{2z+h}{2h}\right)^k, \ -\frac{h}{2} \le z \le \frac{h}{2},$$
$$V_m(z) = 1 - V_c(z). \tag{1}$$

in which subscripts m and c represent the metal and ceramic constituents, respectively.

According to the mentioned law, the Young modulus can be expressed in the form

$$E(z) = E_m + E_{cm}\left(\frac{2z+h}{2h}\right)^k, \ -\frac{h}{2} \le z \le \frac{h}{2}. \tag{2}$$

where the Poisson ratio ν is assumed to be constant $\nu(z) = const$

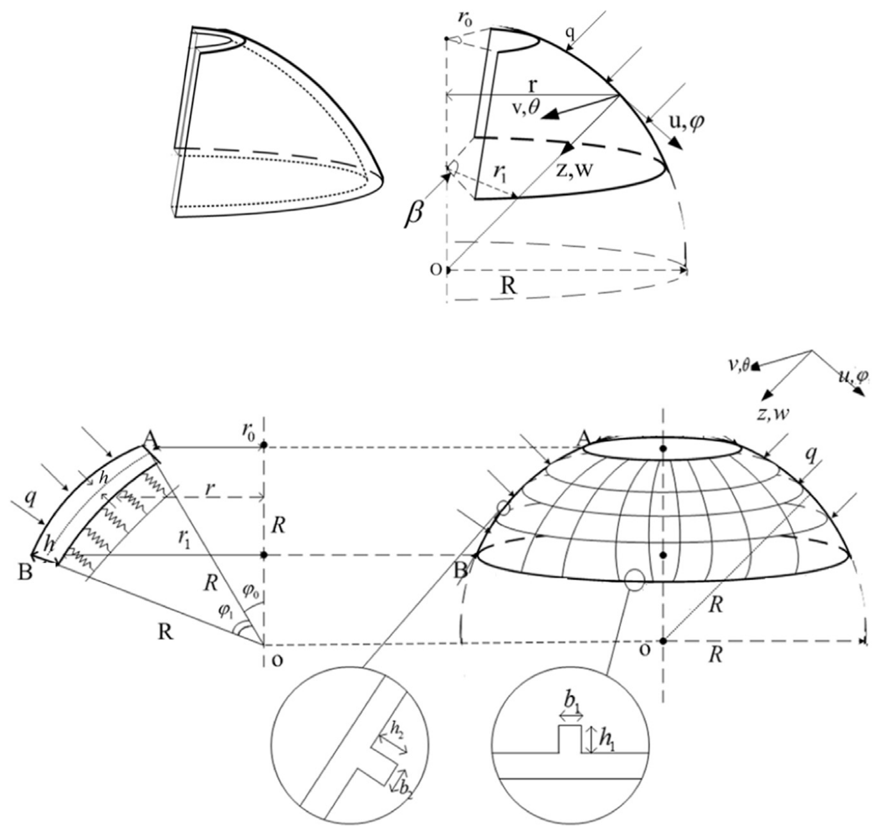

Fig. 1. Configuration of a FGM annular spherical segment shells and eccentrically stiffened FGM annular spherical shell.

and $E_{cm} = E_c - E_m$.

The reaction-deflection relation of Pasternak foundation $q_e = k_1 w - k_2 \Delta w$, where $\Delta w = \frac{\partial^2 w}{\partial r^2} + \frac{1}{r}\frac{\partial w}{\partial r} + \frac{1}{r^2}\frac{\partial^2 w}{\partial \theta^2}$ is a Laplace's operator.

3. Theoretical formulations and stability analysis

For a thin annular spherical segment shells it is convenient to introduce a variable r, referred as the radius of parallel circle with the base of shell and defined by $r = R\sin\varphi$. Moreover, due to shallowness of the shell it is approximately assumed that $\cos\varphi = 1,\ Rd\varphi = dr$.

The strains at the middle surface and the change of curvatures and twist are related to the displacement components u, v, w in the φ, θ, z coordinate directions (where φ and θ are in the meridional and circumferential direction of the shells, respectively and z is perpendicular to the middle surface positive inwards), respectively, taking into account Von Karman – Donnell nonlinear terms as [20,25].

$$\begin{aligned}
\varepsilon_r^0 &= \frac{\partial u}{\partial r} - \frac{w}{R} + \frac{1}{2}\left(\frac{\partial w}{\partial r}\right)^2, & \chi_r &= \frac{\partial^2 w}{\partial r^2},\\
\varepsilon_\theta^0 &= \frac{1}{r}\left(\frac{\partial v}{\partial \theta} + u\right) - \frac{w}{R} + \frac{1}{2r^2}\left(\frac{\partial w}{\partial \theta}\right)^2, & \chi_\theta &= \frac{1}{r}\frac{\partial w}{\partial r} + \frac{1}{r^2}\frac{\partial^2 w}{\partial \theta^2},\\
\gamma_{r\theta}^0 &= \frac{\partial v}{\partial r} + \frac{1}{r}\frac{\partial u}{\partial \theta} - \frac{v}{r} + \frac{1}{r}\frac{\partial w}{\partial r}\frac{\partial w}{\partial \theta}, & \chi_{r\theta} &= \frac{1}{r}\frac{\partial^2 w}{\partial r \partial \theta} - \frac{1}{r^2}\frac{\partial w}{\partial \theta}.
\end{aligned} \tag{3}$$

The nonlinear equilibrium equations of a perfect shell based on the classical shell theory [20].

$$\frac{\partial N_r}{\partial r} + \frac{1}{r}\frac{\partial N_{r\theta}}{\partial \theta} + \frac{N_r}{r} - \frac{N_\theta}{r} = 0, \tag{4}$$

$$\frac{\partial N_\theta}{r\partial \theta} + \frac{\partial N_{r\theta}}{\partial r} + \frac{2N_{r\theta}}{r} = 0, \tag{5}$$

$$\begin{aligned}
&\frac{\partial^2 M_r}{\partial r^2} + \frac{2}{r}\frac{\partial M_r}{\partial r} + 2\left(\frac{\partial^2 M_{r\theta}}{r\partial r\partial \theta} + \frac{1}{r^2}\frac{\partial M_{r\theta}}{\partial \theta}\right) + \frac{1}{r^2}\frac{\partial^2 M_\theta}{\partial \theta^2} - \frac{1}{r}\frac{\partial M_\theta}{\partial r} + \frac{1}{R}(N_r + N_\theta)\\
&\quad + N_r\frac{\partial^2 w}{\partial r^2} - 2N_{r\theta}\left(\frac{1}{r^2}\frac{\partial w}{\partial \theta} - \frac{\partial^2 w}{r\partial r\partial \theta}\right) + N_\theta\left(\frac{1}{r}\frac{\partial w}{\partial r} + \frac{1}{r^2}\frac{\partial^2 w}{\partial \theta^2}\right)\\
&\quad + q - k_1 w + k_2 \Delta w = 0.
\end{aligned} \tag{6}$$

The constitutive stress-strain equations by Hooke law for the shell material are omitted here for brevity. The contribution of stiffeners can be accounted for using the Lekhnitskii smeared stiffeners technique [12–15,28]. Then integrating the stress-strain equations and their moments through the thickness of the shell, the expressions for force and moment resultants of an eccentrically stiffened FGM annular spherical segment are obtained.

$$\begin{Bmatrix} N_r \\ N_\theta \\ N_{r\theta} \\ M_r \\ M_\theta \\ M_{r\theta} \end{Bmatrix} = \begin{bmatrix}
\left(A_{11} + \frac{E_0 A_1}{s_1}\right) & A_{12} & 0 & -(B_{11} + C_1) & -B_{12} & 0\\
A_{12} & \left(A_{22} + \frac{E_0 A_2}{s_2}\right) & 0 & -B_{12} & -(B_{22} + C_2) & 0\\
0 & 0 & A_{66} & 0 & 0 & -2B_{66}\\
(B_{11} + C_1) & B_{12} & 0 & -\left(D_{11} + \frac{E_0 I_1}{s_1}\right) & -D_{12} & 0\\
B_{12} & (B_{22} + C_2)\varepsilon & 0 & -D_{12} & -\left(D_{22} + \frac{E_0 I_2}{s_2}\right) & 0\\
0 & 0 & B_{66} & 0 & 0 & -2D_{66}
\end{bmatrix}
\begin{Bmatrix} \varepsilon_r^0 \\ \varepsilon_\theta^0 \\ \gamma_{r\theta}^0 \\ \chi_r \\ \chi_\theta \\ \chi_{r\theta} \end{Bmatrix} \tag{7}$$

where A_{ij}, B_{ij}, D_{ij}, ($i, j = 1, 2, 6$) are extensional, coupling and bending stiffness of the shell without stiffeners:

$$A_{11} = A_{22} = \frac{E_1}{1-\nu^2};\quad A_{12} = \frac{E_1\nu}{1-\nu^2};\quad A_{66} = \frac{E_1}{2(1+\nu)};$$
$$B_{11} = B_{22} = \frac{E_2}{1-\nu^2};\quad B_{12} = \frac{E_2\nu}{1-\nu^2};\quad B_{66} = \frac{E_2}{2(1+\nu)};$$
$$D_{11} = D_{22} = \frac{E_3}{1-\nu^2};\quad D_{12} = \frac{E_3\nu}{1-\nu^2};\quad D_{66} = \frac{E_3}{2(1+\nu)};$$

with

$$s_1 = \frac{2\pi r}{n_1},\ s_2 = \frac{R\varphi_1 - R\varphi_0}{n_2} = \frac{R}{n_2}\left(\text{arsin}\frac{r_1}{R} - \text{arsin}\frac{r_0}{R}\right);$$

$$C_1 = \frac{E_0A_1z_1}{s_1};\quad C_2 = \frac{E_0A_2z_2}{s_2};$$
$$I_1 = \frac{d_1h_1^3}{12} + A_1z_1^2;\quad z_1 = \frac{h_1+h}{2};\ I_2 = \frac{d_2h_2^3}{12} + A_2z_2^2;\ z_2 = \frac{h_2+h}{2};\tag{8}$$

$$E_1 = \int_{-h/2}^{h/2}\left[E_c + E_{cm}\left(\frac{2z+h}{h}\right)^k\right]dz = hE_m + \frac{hE_{cm}}{k+1},$$
$$E_2 = \int_{-h/2}^{h/2}z\left[E_c + E_{cm}\left(\frac{2z+h}{h}\right)^k\right]dz = h^2E_{cm}\left(\frac{1}{k+2} - \frac{1}{2k+2}\right),$$
$$E_3 = \int_{-h/2}^{h/2}z^2\left[E_c + E_{cm}\left(\frac{2z+h}{h}\right)^k\right]dz = \frac{h^3E_m}{12} + \frac{h^3E_{cm}}{2(k+1)(k+2)(k+3)}.\tag{9}$$

Substitution of (Eqs. (3) and 7) into (Eqs. (4)–6) gives 3 nonlinear equations of u, v, w.

In this study, an analytical approach is used to investigate the nonlinear stability of FGM annular spherical segment resting on elastic foundations under external pressure. The FGM annular spherical segment is assumed to be simply supported along the periphery and subjected to external pressure uniformly distributed on the outer surface of the shell. Depending on the inplane behavior at the edge of boundary conditions will be considered in cases the edges are simply supported, immovable and movable.

Case A: The edges of the annular spherical segment are simply supported and movable. For this case, the boundary conditions are expressed by

$$w = 0,\ \ M_r = 0,\ \ N_r = 0,\ \ N_{r\theta} = 0,\ \text{at } r = r_0$$
$$w = 0,\ \ M_\theta = 0,\ \ N_\theta = 0,\ \ N_{r\theta} = 0,\ \text{at } \theta = 0, \beta\tag{10}$$

From boundary conditions (10) approximate solutions for the nonlinear equations of u, v, w are assumed as

$$u = U\cos\frac{m\pi(r-r_0)}{r_1-r_0}\sin\left(\frac{n\pi\theta}{\beta}\right);$$

$$v = V\sin\frac{m\pi(r-r_0)}{r_1-r_0}\cos\left(\frac{n\pi\theta}{\beta}\right);$$
$$w = W\sin\frac{m\pi(r-r_0)}{r_1-r_0}sin\left(\frac{n\pi\theta}{\beta}\right).\tag{11}$$

where m, n are numbers of half waves in meridional and circumferential direction, respectively.

Subsequently, introduction of solutions (11) into obtained 3 nonlinear equations of u, v, w, we obtain the equations, which have form

$$R_1(u, v, w) = 0,$$
$$R_2(u, v, w) = 0,$$
$$R_3(u, v, w) = 0,$$

Applying Galerkin method for the resulting, that are

$$\int_{r_0}^{r_1}\int_0^\beta R_1\cos\frac{m\pi(r-r_0)}{r_1-r_0}\sin(n\theta)rdrd\theta = 0;$$
$$\int_{r_0}^{r_1}\int_0^\beta R_2\sin\frac{m\pi(r-r_0)}{r_1-r_0}cos(n\theta)rdrd\theta = 0,$$
$$\int_{r_0}^{r_1}\int_0^\beta R_3sin\frac{m\pi(r-r_0)}{r_1-r_0}\sin(n\theta)rdrd\theta = 0.\tag{12}$$

we obtain the following equations

$$a_{11}U + a_{12}V + a_{13}W + a_{14}W^2 = 0,$$
$$a_{21}U + a_{22}V + a_{23}W + a_{24}W^2 = 0,$$
$$a_{31}U + a_{32}V + a_{33}W + (a_{34}U + a_{35}V + k_1a_{36} + k_2a_{37})$$
$$W + a_{38}W^2 + a_{39}W^3 + a_{310}q = 0,\tag{13}$$

where the detail of coefficients a_{ij} notation may be found in Appendix. A.

Eq. (13) allows determine the deflection curve equation with form

$$q = c_{11}W^3 + c_{12}W^2 + c_{13}W + (c_{14}k_1 + c_{15}k_2)W.\tag{14}$$

with

$$c_{11} = \frac{a_{34}b_2 + a_{35}b_4 + a_{39}}{-a_{310}};$$
$$c_{12} = \frac{a_{31}b_2 + a_{32}b_4 + a_{34}b_1 + a_{35}b_3 + a_{38}}{-a_{310}};$$
$$c_{13} = \frac{a_{31}b_1 + a_{32}b_3 + a_{33}}{-a_{310}};\quad c_{14} = \frac{a_{36}}{-a_{310}};$$
$$c_{15} = \frac{a_{37}}{-a_{310}};\ b_1 = \frac{a_{13}a_{22} - a_{23}a_{12}}{a_{12}a_{21} - a_{11}a_{22}};\quad b_2 = \frac{a_{14}a_{22} - a_{24}a_{12}}{a_{12}a_{21} - a_{11}a_{22}};$$
$$b_3 = \frac{a_{13}a_{21} - a_{23}a_{11}}{a_{11}a_{22} - a_{12}a_{21}};\quad b_4 = \frac{a_{14}a_{21} - a_{24}a_{11}}{a_{11}a_{22} - a_{12}a_{21}};$$

Eq. (14) is used for determining the nonlinear stability of eccentrically stiffened functionally graded annular spherical segment under uniform external pressure in case when the edges of the annular spherical segment are simply supported and movable. For given values of the material and geometrical properties of the FGM annular segment, critical loads are determined by minimizing loads with respect to values of m, n.

Case B: The edges of the annular spherical segment are simply supported and immovable. For this case, the boundary conditions are expressed by

$$u = 0,\ \ w = 0,\ \ M_r = 0,\ \ N_r = 0,\ \ N_{r\theta} = 0,\ \text{at } r = r_0$$
$$w = 0,\ \ M_\theta = 0,\ \ N_\theta = 0,\ \ N_{r\theta} = 0,\ \text{at } \theta = 0, \beta\tag{15}$$

With boundary conditions (15), the approximate solutions for the nonlinear equations of u, v, w are assumed as

$$u = Usin\frac{m\pi(r-r_0)}{r_1-r_0}cos\left(\frac{n\pi\theta}{\beta}\right);$$
$$v = V\cos\frac{m\pi(r-r_0)}{r_1-r_0}\sin\left(\frac{n\pi\theta}{\beta}\right);$$
$$w = W\sin\frac{m\pi(r-r_0)}{r_1-r_0}sin\left(\frac{n\pi\theta}{\beta}\right).\tag{16}$$

Completely similar to the first case, the equation allows determining load deflection curve of the similar form

$$q = g_{11}W^3 + g_{12}W^2 + g_{13}W + (g_{14}k_1 + g_{15}k_2)W.\tag{17}$$

with

Table 1
The critical loads $q_{cr} \times 10(\mathrm{MPa})$ of eccentrically stiffened functionally graded annular spherical segment under uniform external pressure.

k	Phuong [20]	Case A	Case B
0	1.3859	1.3613	1.4062
1	0.7485	0.7378	0.7503
5	0.4508	0.4317	0.4632

$$g_{11} = \frac{t_{34}l_2 + t_{35}l_4 + t_{39}}{-t_{310}}; \quad g_{12} = \frac{t_{31}l_2 + t_{32}l_4 + t_{34}l_1 + t_{35}l_3 + t_{38}}{-t_{310}};$$
$$g_{13} = \frac{t_{31}l_1 + t_{32}l_3 + t_{33}}{-t_{310}}; \quad g_{14} = \frac{t_{36}}{-t_{310}};$$
$$g_{15} = \frac{t_{37}}{-t_{310}}; \; l_1 = \frac{t_{13}t_{22} - t_{23}t_{12}}{t_{12}t_{21} - t_{11}t_{22}}; \quad l_2 = \frac{t_{14}t_{22} - t_{24}t_{12}}{t_{12}t_{21} - t_{11}t_{22}};$$
$$l_3 = \frac{t_{13}t_{21} - t_{23}t_{11}}{t_{11}t_{22} - t_{12}t_{21}}; \quad l_4 = \frac{t_{14}t_{21} - t_{24}t_{11}}{t_{11}t_{22} - t_{12}t_{21}};$$

and the detail of coefficients t_{ij} are given in Appendix. B.

Eq. (17) is used for determining the nonlinear stability of eccentrically stiffened functionally graded annular spherical segment under uniform external pressure in case when the edges of the annular spherical segment are simply supported and immovable.

4. Results and discussion

The nonlinear stability of eccentrically stiffened functionally graded annular spherical segment is analyzed in this section. The shell consists of aluminum (metal) and alumina (ceramic) with the Young modulus of Aluminum is $E_m = 70 \times 10^9$ Pa, and alumina $E_c = 380 \times 10^9$ Pa. The Poisson's ratio is chosen to be $\nu = 0.3$ for simplicity.

4.1. Comparison study

To validate the proposed approach, the critical loads of eccentrically stiffened functionally graded annular spherical segment with elastic foundations are compared with the known results in the literature. There has not been any publication from the open literature about eccentrically stiffened annular spherical segment. As such, the study is conducted a comparison with the critical load of functionally graded annular spherical segment under uniform external pressure [24] by Phuong in the same conditions and geometrical parameters, the results are presented in Table 1. The critical load changes are calculated by closed-form relation (14) and (17) with

$R/h = 800, \;\; \beta = \pi/6, \; r_0/R = 0.2, \;\; r_1/R = 0.5, \;\; (m, n) = (5, 1).$

As can be seen in Table 1, the good agreement in the comparison verified the accuracy of the present approach in this paper.

4.2. The influence of the initial conditions and geometry parameters on nonlinear stability of FGM annular spherical segment with eccentrically stiffened

To illustrate the present approach, consider a FGM annular spherical segment with eccentrically stiffened. The geometric parameters of annular and stiffeners considered here are [24] $d_1 = d_2 = 0.002\,m, \;\; h_1 = h_2 = 0.005\,m, \;\; n_1 = \;\; n_2 = 30, R = 2\,m$. Unless there wise specified, the inside stiffeners of the shell is ceramic-rich and the outside stiffeners is metal-rich. In case no mention the inside or outside stiffeners mean is calculated for the inside stiffeners in ceramic.

Table 2 show the effects of open angle β, volume fraction index k and ratio R/h on the critical loads $q_{cr}(\mathrm{MPa})$of annular spherical segments under external pressure without elastic foundations. It is evident that critical loads decrease when the volume of these parameter increases in case B. ie in cases when the edges of the annular spherical segment are simply supported and immovable, but in case A when the edges of the annular spherical segment are simply supported and movable, the critical loads only decrease when the volume of these parameter increases when the open angle $\beta < \pi/2$, when $\beta > \pi/2$ the critical loads decrease when the volume of R/h decrease.

Effects of the elastic foundations (K_1, K_2) and mode (m, n) on the critical loads q_{cr} of FGM annular spherical segments are shown in

Table 2
Effects of open angle β, volume fraction index k and ratio R/h on the critical loads $q_{cr}(\mathrm{MPa})$of annular spherical segments under without elastic foundations (case A).

R/h	β	$\pi/15$	$\pi/12$	$\pi/6$	$\pi/3$	$\pi/2$	$2\pi/3$
	k	$r_0/R = 0.05, \;\; r_1/R = 0.5, \;\; (m, n) = (5, 1)$					
800	0	0.6856(A)	0.8626(A)	1.3955(A)	1.3667(A)	1.0889(A)	0.8134(A)
		0.9228(B)	1.2321(B)	2.0931(B)	2.3102(B)	2.3382(B)	2.3467(B)
	1	0.3292(A)	0.4067(A)	0.6531(A)	0.6575(A)	0.5405(A)	0.4199(A)
		0.3616(B)	0.5080(B)	0.9397(B)	1.0675(B)	1.0873(B)	1.0938(B)
	5	0.1814(A)	0.2168(A)	0.3388(A)	0.3432(A)	0.2857(A)	0.2256(A)
		0.1927(B)	0.2650(B)	0.4818(B)	0.5474(B)	0.5578(B)	0.5613(B)
1000	0	0.4738(A)	0.6259(A)	1.0635(A)	1.0482(A)	0.8326(A)	0.6182(A)
		0.6502(B)	0.9014(B)	1.5997(B)	1.7824(B)	1.8071(B)	1.8147(B)
	1	0.2366(A)	0.3082(A)	0.5206(A)	0.5245(A)	0.4273(A)	0.3276(A)
		0.2684(B)	0.3927(B)	0.7554(B)	0.8631(B)	0.8798(B)	0.8852(B)
	5	0.1289(A)	0.1635(A)	0.2706(A)	0.2742(A)	0.2256(A)	0.1752(A)
		0.1403(B)	0.2027(B)	0.3884(B)	0.4448(B)	0.4537(B)	0.4567(B)
1200	0	0.3610(A)	0.4925(A)	0.8624(A)	0.8530(A)	0.6764(A)	0.5005(A)
		0.5020(B)	0.7130(B)	1.2992(B)	1.4556(B)	1.4772(B)	1.4839(B)
	1	0.1855(A)	0.2502(A)	0.4355(A)	0.4387(A)	0.3553(A)	0.2701(A)
		0.2168(B)	0.3244(B)	0.6360(B)	0.7283(B)	0.7425(B)	0.7472(B)
	5	0.1005(A)	0.1325(A)	0.2272(A)	0.2299(A)	0.1877(A)	0.1442(A)
		0.1123(B)	0.1672(B)	0.3284(B)	0.3772(B)	0.3849(B)	0.7472(B)

(A): case A; (B): case B

Table 3
Effects of the elastic foundations (K_1, K_2) and mode (m, n) on the critical loads $q_{cr}(\text{MPa})$ of annular spherical segments under external pressure.

(K_1, K_2) (m, n)	(0,0) $R/h = 800,\ r_0/R = 0.05,\ r_1/R = 0.5,\ \beta = \pi/6,\ k = 1.$	(10,0)	(100,10)	(0,10)	(10,20)
(1,1)	0.2302 (A)	1.3279 e5 (A)	1.3272 e6 (A)	74.1165 (A)	1.3286 e5 (A)
	−6.2012 (B)	3.8912 e6 (B)	4.2804 e7 (B)	3.8912 e6 (B)	1.1673 e7 (B)
(5,1)	0.6531(A)	2.2487 e5 (A)	2.2441 e6 (A)	516.0362 (A)	2.3467 e4 (A)
	1.0938 (B)	2.8529 e5 (B)	3.1382 e6 (B)	2.8529 e5 (B)	8.5587 e5 (B)
(9,1)	0.4313 (A)	0.6834 e5 (A)	0.6838 e6 (A)	448.7510 (A)	6.9242 e4 (A)
	0.5935 (B)	0.8949 e5 (B)	0.9844 e5 (B)	8.9499 e4 (B)	2.6849 e5 (B)
(1,3)	0.5813 (A)	1.0258 e5 (A)	1.0263 e6 (A)	434.1690 (A)	1.0345 e5 (A)
	10.2791 (B)	1.9897 e6 (B)	2.1887 e7 (B)	1.9897 e6 (B)	5.9692 e6 (B)
(1,5)	1.9205 (A)	0.7404 e5 (A)	0.7413 e6 (A)	858.3343 (A)	0.7576 e5 (A)
	5.6218 (B)	1.0608 e6 (B)	1.1669 e7 (B)	1.0608 e6 (B)	3.1825 e6 (B)

Table 4
Effects of the number, type and position of stiffeners and elastic foundations on nonlinear static response of the FGM annular spherical segment.

(K_1, K_2) (n_1, n_2)	$(K_1 = 0, K_2 = 0)$ $R/h = 800,\ \beta = \pi/12,\ r_0/R = 0.05,\ r_1/R = 0.5,\ (m, n) = (3, 1).$	$(K_1 = 50, K_2 = 20)$
(0,0)	0.7152 (A)	3.4952 e5 (A)
	0.7248 (B)	3.6361 e5 (B)
(30,0)	0.4782 (A)	3.7823 (A)
	0.4725 (B)	3.7983 (B)
(0,30)	−0.137 (A)	−3.685 e5 (A)
	−0.1169 (B)	−3.321 e2 (B)
(30,30)	0.2752 (A)	6.2376 e5 (A)
	0.4067 (B)	6.6254 e2 (B)

Table 3. Obviously, the elastic foundations and mode (m, n) played positive role on nonlinear static response of the FGM annular spherical segment: the large K_1 and K_2 cloefficients are, the larger loading capacity of the shells is and more influence in the case B clearer than A; whereas effects of mode (m, n) seems not to follow any rules. It is clear that the elastic foundations can enhance the mechanical loading capacity for the FGM annular spherical segments, and the effect of Pasternak foundation K_2 on critical uniform external pressure is bigger than the Winkler foundation K_1.

Effects of the number, type and position of stiffener and elastic foundations on nonlinear static response of the FGM annular spherical segment with and without eccentrically stiffened are presented in Table 4. ($q_{cr}(\text{MPa})$).

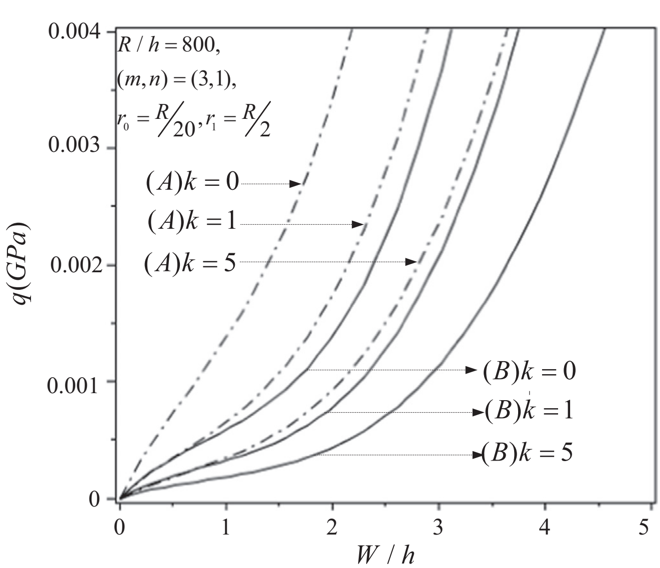

Fig. 2. Effects of volume fraction index k on the nonlinear stability of eccentrically stiffened functionally graded annular spherical segment.

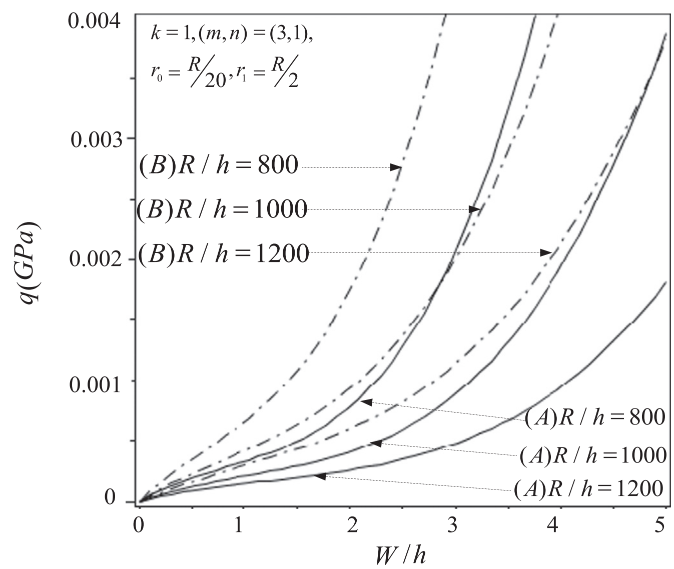

Fig. 3. Effects of curvature radius-thickness ratio on the nonlinear stability of eccentrically stiffened functionally graded annular spherical segment.

The effects of material and geometric parameters on the nonlinear stability of eccentrically stiffened functionally graded annular spherical segment (without effect of elastic foundations $K_1 = K_2 = 0$) are presented in Figs. 2 and 3. It is noted that in all figures W/h denotes the dimensionless maximum deflection of the shell.

Fig. 2 shows the effects of volume fraction index $k(0, 1, 5)$ on the nonlinear stability of eccentrically stiffened functionally graded annular spherical segment subjected to external pressure (mode $(m, n) = (3, 1)$). As can be seen, the load–deflection curves become lower when k increases.

Fig. 3 depicts the effects of curvature radius - thickness ratio R/h (800, 1000 and 1200) on the nonlinear behavior of the external pressure of eccentrically stiffened functionally graded annular spherical segment (mode $(m, n) = (3, 1)$). From Fig. 3 we can conclude that when the annular spherical segments get thinner - corresponding with R/h getting bigger, the critical buckling loads will get smaller.

5. Concluding remarks

The present paper aims to propose a nonlinear analysis of eccentrically stiffened FGM annular spherical segment shells on elastic foundations under uniform external pressure. Approximate solutions are assumed to satisfy the simply supported boundary condition and Galerkin method is applied to obtain closed-form relations of bifurcation type of nonlinear stability. The effects of material, geometrical properties, elastic foundations, combination of external pressure and stiffener arrangement, stiffener number on the nonlinear stability of eccentrically stiffened FGM annular spherical segment are analyzed and discussed.

Acknowledgement

This work was supported by the Grant in Mechanics of the National Foundation for Science and Technology Development of Vietnam – NAFOSTED code 107.02-2015.03. The authors are grateful for this support.

Appendix A

$$a_{11} = \frac{\pi^2 m^2\left[3\pi A_{11}\left(r_1^3 + r_0^2 r_1 + r_0 r_1^2 + r_0^3\right) + 2E_0 A_1 n_1\left(r_1^2 + r_0 r_1 + r_0^2\right)\right]}{48(r_0 - r_1)} + \frac{n^2\pi A_{66}\left(r_0^2 - r_1^2\right)}{8} + \frac{\pi\left(r_0^2 - r_1^2\right)(A_{11} + 2A_{22})}{16} + \frac{\pi E_0 A_2\left(r_0^2 - r_1^2\right)}{8s_2},$$

$$a_{12} = -\frac{1}{12}\pi^2 mn\left(r_1^2 + r_0 r_1 + r_0^2\right)(A_{12} + A_{66}) - \frac{n(-r_1 + r_0)^2(A_{12} + 2A_{66} + A_{22})}{8m} - \frac{n(-r_1 + r_0)^2 E_0 A_2}{8ms_2},$$

$$a_{13} = \frac{n^2\pi^3 m(r_1 + r_0)(B_{12} + 2B_{66})}{8\beta} + \frac{\pi^2 m^3\left[3\pi\beta B_{11}(r_1 + r_0)\left(r_1^2 + r_0^2\right) + 2E_0 A_1 z_1 n_1\left(r_1^2 + r_0 r_1 + r_0^2\right)\beta\right]}{48(-r_1 + r_0)^2} + - \frac{\left[3\pi\beta m(r_1 + r_0)\left(r_1^2 + r_0^2\right)(A_{11} + A_{12}) + 2E_0 A_1 n_1 m\beta\left(r_1^2 + r_0 r_1 + r_0^2\right) + 3m\pi\beta(3A_{12} + 2A_{22} + A_{11})(r_1 + r_0)(-r_1 + r_0)^2\right]}{48R} + \frac{m\pi\beta(B_{11} + 2B_{22})(r_1 + r_0)}{16} + - \frac{(r_1 + r_0)(-r_1 + r_0)^2 E_0 A_2 \beta}{8m\pi R s_2},$$

$$a_{14} = \left(-r_0 + r_0(-1)^n + r_1(-1)^m - r_1(-1)^{n+m}\right)\left(\frac{-A_{12}n\pi}{9\beta} + \frac{A_{66}n\pi}{9\beta} - \frac{14A_{12}\beta}{27n\pi} + \frac{14A_{11}\beta}{n\pi}\right) + \frac{\beta m^2\left(1 - (-1)^n\right)\left(n_1 E_0 A_2\left((-1)^m r_1^2 - r_0^2\right) + 2A_{11}\pi\left((-1)^m r_1^3 - r_0^3\right)\right)}{9(-r_1 + r_0)^2} - \frac{7n_1 E_0 A_1 \beta((-1)^n + (-1)^m - (-1)^{(n+m)} - 1)}{162},$$

$$a_{21} = -\frac{\pi^2 mn\left(r_1^2 + r_0 r_1 + r_0^2\right)(A_{12} + A_{66})}{12} + \frac{n(-r_1 + r_0)^2(A_{12} - A_{22})}{8m} - \frac{nE_0 A_2(-r_1 + r_0)^2}{8ms_2},$$

$$a_{22} = \frac{n^2\pi^2\left(r_0^2 - r_1^2\right)A_{22}}{8\beta} + \frac{A_{66}\beta\pi^2 m^2(r_1 + r_0)\left(r_0^2 + r_1^2\right)}{16(-r_1 + r_0)} + \frac{\beta A_{66}\left(r_0^2 - r_1^2\right)}{16} + \frac{n^2\pi^2 E_0 A_2\left(r_0^2 - r_1^2\right)}{8\beta s_2},$$

$$a_{23} = -\frac{\pi^3 n^3(-r_1 + r_0)(B_{22} + C_2)}{4\beta^2} - \frac{m^2 n\pi^3\left(r_1^2 + r_0 r_1 + r_0^2\right)(B_{12} + 2B_{66})}{12(-r_1 + r_0)} - \frac{n(-r_1 + r_0)^3(A_{22} + A_{12})}{8\pi m^2 R} + + \frac{\pi n E_0 A_2\left(r_0^3 - r_1^3\right)}{12Rs_2} - \frac{nE_0 A_2(-r_1 + r_0)^3}{8\pi m^2 R s_2} + \frac{\pi n(-r_1 + r_0)\left[2(A_{22} + A_{12})\left(r_1^2 + r_0 r_1 + r_0^2\right) + 3R(B_{12} - B_{22} - C_2)\right]}{24R},$$

$$a_{24} = \frac{m\pi\left(1 - (-1)^n\right)\left((-1)^m r_1 - r_0\right)(A_{12} - A_{66})}{9(-r_1 + r_0)} - (-r_1 + r_0)\left(1 - (-1)^n\right)\left(1 + (-1)^m\right)\frac{2n^2\pi A_{22}}{9m\beta^2}\left(1 - \frac{1}{s_2}\right) - \frac{2\left(1 - (-1)^n\right)(-r_1 + r_0)}{81\pi m}\left(7A_{12}\left(1 + (-1)^m\right) + 10A_{66}\left(1 - (-1)^m\right)\right),$$

$$a_{31} = \frac{m\pi(r_1^2 + r_0 r_1 + r_0^2)}{12}\left[\frac{(2B_{66} + B_{12})\pi^2 n^2}{\beta} + \beta(C_2 + \beta B_{22})\right] + \frac{\beta\pi^2 n_1 z_1 m^3 A_1 E_0(r_0 + r_1)(r_1^2 + r_0^2)}{32(-r1 + r0)^2} + - (-r_1 + r_0)^2\left[\frac{\pi n^2(-B_{22} + 2B_{66} - C_2 + B_{12})}{8m\beta} - \frac{\beta(B_{22} + C_2)}{4m\pi}\right] + \frac{\beta A_1 m E_0 n_1(r_0 + r_1)(-r_0^2 + z_1 R - r_1^2)}{32R} + + \frac{\beta}{8}(r_1^2 + r_0 r_1 + r_0^2)(-r_1 + r_0)^2\left(\frac{-A_{22} + A_{12} + 2A_{11}}{mR\pi} - \frac{E_0 A_2}{s2mR\pi}\right) + \frac{3\beta(-r_1 + r_0)^4}{16m^3 R\pi^3}\left(\frac{E_0 A_2}{s_2} + A_{22} - A_{12} - 2A_{11}\right) + + \frac{m\pi\beta}{20}\left(r_1^4 + r_0 r_1^3 + r_0^2 r_1^2 + r_0^3 r_1 + r_0^4\right)\left(-\frac{(A_{12} + A_{11})}{R} + \frac{\pi^2 m^2 B_{11}}{(-r_1 + r_0)^2}\right) + \frac{3(-r_1 + r_0)^2 E_0 n_1(r_1 + r_0)\beta A_1}{32\pi^2 mR},$$

$$a_{32} = -\frac{n^3(B_{22} + C_2)\pi^3(r_0^2 - r_1^2)}{8\beta^2} + \frac{\pi n(r_0^2 - r_1^2)}{16R}\left((r_0^2 + r_1^2)(A_{22} + A_{12}) + 4RC_3 + 3B_{12}R + 6B_{66}R + 4RB_{22}\right) + - \frac{\pi^3(r_0 + r_1)(r_0^2 + r_1^2)(2B_{66} + B_{12})m^2 n}{16(r_0 - r_1)} - \frac{3n(r_0 + r_1)(r_0 - r_1)^3(A_{12} + A_{22})}{16m^2 R\pi} + \frac{E_0 A_2 \pi n(r_0^4 - r_1^4)}{16Rs_2} - \frac{3(r_0 + r_1)(r_0 - r_1)^3 E_0 A_2 n}{16m^2 R\pi s_2};$$

$$
\begin{aligned}
a_{33} = &\left(\frac{-(r_0 - r_1)E_0}{2s_2}\left(\frac{\beta}{2n} + \frac{\pi^2 n^2}{\beta}\right) + \frac{m^2(r_1^2 + r_0 r_1 + r_0^2)\pi^2 E_0 \beta}{12(r_0 - r_1)ns_2}\right.\\
&\left.+ \frac{n^4(r_0 - r_1)\pi^4 E_0}{4\beta^3 s_2}\right)I_2\\
&+ \left(\frac{m^2(r_0 + r_1)n_1 E_0 \pi\beta}{32(r_0 - r_1)} + \frac{\beta\pi^3 E_0 n_1 (r_0 + r_1)(r_1^2 + r_0^2)m^4}{32(r_0 - r_1)^3}\right)I_1\\
&- \frac{(r_0 - r_1)\pi^2 n^2 \beta D_{66}}{2} + \frac{\beta\pi^4(r_0^4 + r_0 r_1^3 + r_0^2 r_1^2 + r_1^4 + r_0^3 r_1)m^4 D_{11}}{20(r_0 - r_1)^3}\\
&+ \left(\frac{n^4(r_0 - r_1)\pi^4}{4\beta^3} - \frac{(r_0 - r_1)\pi^2 n^2}{2\beta} - \frac{(r_0 - r_1)\beta}{4}\right.\\
&\left.+ \frac{m^2(r_1^2 + r_0 r_1 + r_0^2)\beta\pi^2}{12(r_0 - r_1)}\right)D_{22} + \frac{(r_0 - r_1)^3(2B_{22} + 2C_2)n^2}{4\beta R m^2}\\
&+ \left(\frac{(r_0 - r_1)(r_0^4 + r_0 r_1^3 + r_0^2 r_1^2 + r_1^4 + r_0^3 r_1)\beta}{20R^2}\right.\\
&\left.- \frac{(r_0 - r_1)^3(r_1^2 + r_0 r_1 + r_0^2)\beta}{4\pi^2 m^2 R^2} + \frac{3(r_0 - r_1)^5\beta}{8m^4 R^2 \pi^4}\right)A_{22}\\
&+ \left(\frac{(r_0 - r_1)^3}{Rm^2}\left(\frac{n^2}{2\beta} - \frac{3\beta}{8\pi^2}\right) + \frac{(r_0 - r_1)(r_1^2 + r_0 r_1 + r_0^2)}{2R}\left(\frac{\beta}{2} - \frac{\pi^2 n^2}{3\beta}\right)\right.\\
&\left.- \frac{m^2(r_0^4 + r_0 r_1^3 + r_0^2 r_1^2 + r_1^4 + r_0^3 r_1)\beta\pi^2}{10(r_0 - r_1)R}\right)B_{12}\\
&+ \left(-\frac{3(r_0 - r_1)^3\beta}{8\pi^2 R m^2} - \frac{m^2(r_0^4 + r_0 r_1^3 + r_0^2 r_1^2 + r_1^4 + r_0^3 r_1)\beta\pi^2}{10(r_0 - r_1)R}\right.\\
&\left.+ \frac{(r_0 - r_1)(r_1^2 + r_0 r_1 + r_0^2)\beta}{4R}\right)B_{11}\\
&+ \left(-\frac{(r_0 - r_1)^3(r_1^2 + r_0 r_1 + r_0^2)\beta}{2\pi^2 m^2 R^2} + \frac{3(r_0 - r_1)^5\beta}{4m^4 R^2 \pi^4}\right.\\
&\left.+ \frac{(r_0 - r_1)(r_0^4 + r_0 r_1^3 + r_0^2 r_1^2 + r_1^4 + r_0^3 r_1)\beta}{10R^2}\right)A_{12}\\
&+ \left(\frac{(r_0 - r_1)(r_0^4 + r_0 r_1^3 + r_0^2 r_1^2 + r_1^4 + r_0^3 r_1)\beta}{20R^2}\right.\\
&\left.- \frac{(r_0 - r_1)^3(r_1^2 + r_0 r_1 + r_0^2)\beta}{4\pi^2 m^2 R^2} + \frac{3(r_0 - r_1)^5\beta}{8m^4 R^2 \pi^4}\right)A_{11}\\
&+ (\left(\frac{(r - r_1)(r_0^4 + r_0 r_1^3 + r_0^2 r_1^2 + r_1^4 + r_0^3 r_1)E_0\beta}{20R^2 n s_2}\right.\\
&\left.- \frac{(r_0 - r_1)^3(r_1^2 + r_0 r_1 + r_0^2)E_0\beta}{4\pi^2 m^2 R^2 s_2} + \frac{3(r_0 - r_1)^5\beta E_0}{8m^4 R^2 \pi^4 n s_2}\right)A_2\\
&+ \left(-\frac{3(r_0 - r_1)^3 E_0 n_1 (r_0 + r_1)\beta}{32\pi^3 m^2 R^2}\right.\\
&+ \frac{(r_0 - r_1)E_0 n_1 (r_0 - r_1)(r_1^2 + r_0 r_1 + r_0^2)\beta}{32\pi R^2}\\
&\left.- \frac{m^2(r_0 + r_1)(r_1^2 + r_0^2)\beta n_1 z_1 E_0 \pi}{16(r_0 - r_1)R}\right)A_1\\
&+ \left(-\frac{(r_0 - r_1)(r_1^2 + r_0 r_1 + r_0^2)\pi^2 C_2}{6\beta R} - \frac{(r_0 - r_1)\pi^2 D_{12}}{\beta}\right.\\
&\left.- \frac{(r_0 - r_1)(r_1^2 + r_0 r_1 + r_0^2)\pi^2 B_{22}}{6\beta R}\right)n^2;
\end{aligned}
$$

$$
\begin{aligned}
a_{34} = &\left(\frac{16(r_0 - r_1)^2\big((-1)^n - 1\big)\big((-1)^m - 1\big)n}{81\beta\pi m^2}\right.\\
&\left.- \frac{2\big((-1)^n - 1\big)\big(r_0^2 + r_1^2(-1)^m\big)\pi n}{9\beta}\right)A_{66}\\
&+ \left(\frac{80(r_0 - r_1)^2\big((-1)^n - 1\big)\big((-1)^m - 1\big)}{81\pi}\left(\frac{2\beta}{\pi^2 n} + \frac{n}{\beta m^2}\right)\right.\\
&\left.- \frac{4\big((-1)^n - 1\big)\big(r_0^2 + r_1^2(-1)^m\big)}{9}\left(\frac{\pi n}{\beta} + \frac{4\beta}{\pi n}\right)\right)A_{12}\\
&+ \left(-\frac{4(r_0 - r_1)^2\big((-1)^n - 1\big)\big((-1)^m - 1\big)E_0 n}{27 s_2 \beta\pi m^2}\right.\\
&\left.- \frac{2\big((-1)^n - 1\big)\big(r_0^2 + r_1^2(-1)^m\big)\beta E_0}{9 s_2 \pi n}\right)A_2\\
&+ \left(-\frac{2\big((-1)^n - 1\big)\big(r_0^2 + r_1^2(-1)^m\big)\beta}{9\pi n}\right.\\
&\left.+ \frac{4(r_0 - r_1)^2\big((-1)^n - 1\big)\big((-1)^m - 1\big)}{27\pi}\left(\frac{7\beta}{3\pi^2 n} - \frac{n}{\beta m^2}\right)\right)A_{22}\\
&+ \left(\frac{160\big((-1)^n - 1\big)\big(r_0^2 + r_1^2(-1)^m\big)\beta}{27\pi n}\right.\\
&- \frac{2912(r_0 - r_1)^2\big((-1)^n - 1\big)\big((-1)^m - 1\big)\beta}{243\pi^3 n}\\
&\left.- \frac{4\big((-1)^n - 1\big)\big(r_0^4 + r_1^4(-1)^m\big)m^2}{9(r_0 - r_1)^2 n}\right)A_{11}\\
&+ \left(\frac{40\big((-1)^n - 1\big)\big(r_0 + r_1(-1)^m\big)\beta n_1 E_0}{27n\pi^2}\right.\\
&\left.- \frac{2\beta n_1 E_0\big((-1)^n - 1\big)\big(r_0^3 + r_1^3(-1)^m\big)}{9(r_0 - r_1)^2 n}\right)A_1
\end{aligned}
$$

$$
\begin{aligned}
a_{35} = &\frac{-4(r_0 - r_1)\big((-1)^n - 1\big)\big(r_0 + r_1(-1)^m\big)}{9m}\left(\frac{\pi n^2}{\beta^2} + \frac{2}{3\pi}\right)A_{22}\\
&- \frac{4(r_0 - r_1)\big((-1)^n - 1\big)\big(r_0 + r_1(-1)^m\big)E_0}{9 s_2 m}\left(\frac{\pi n^2}{\beta^2} - \frac{2_0}{3\pi}\right)A_2 +\\
&+\left(-\frac{4\pi\big((-1)^n - 1\big)\big(r_0^3 + r_1^3(-1)^m\big)m}{9(r_0 - r_1)}\right.\\
&\left.+ \frac{80(r_0 - r_1)\big((-1)^n - 1\big)\big(r_0 + r_1(-1)^m\big)}{27Pi*m}\right)A_{12}\\
&- \frac{2\pi m\big((-1)^n - 1\big)\big(r_0^3 + r_1^3(-1)^m\big)A_{66}}{9(r_0 - r_1)};
\end{aligned}
$$

$$a_{36} = \frac{3\beta(-r_1+r_0)^5}{8m^4\pi^4} - \frac{(-r_1+r_0)^2\left(r_0^3-r_1^3\right)\beta}{4m^2\pi^2} + \frac{\pi\beta(-r_1+r_0)^5}{20},$$

$$\begin{aligned} a_{37} = {} & \frac{\beta\left(r_0^3-r_1^3\right)}{8} - \frac{m^2\pi^2\beta\left(r_0^4+r_0^2r_1^2+r_0r_1^3+r_0^3r_1+r_1^4\right)}{20(-r_1+r_0)} - \frac{3(-r_1+r_0)^3\beta}{16\pi^2m^2} \\ & + \frac{\pi^2n^2\left(r_0^3-r_1^3\right)}{12\beta} - \frac{(-r_1+r_0)^3n^2}{4\beta m^2}. \end{aligned}$$

$$a_{39} = \left(\begin{aligned} & \frac{3n(r_0-r_1)(A_{22}s_2+E_0A_2)\pi^4}{128\beta^3s_2} - \frac{n^2(r_0-r_1)(-3A_{22}s_2+9A_{12}s_2+10A_{66}s_2-3E_0A_2)\pi^2)}{512\beta s_2} \\ & + \frac{9(-r_1+r_0)(A_{11}-17A_{12})\beta}{4096} \\ & \quad + \frac{3\beta\pi^3m^4}{5120(r_0-r_1)^3} \\ & \quad \left(\begin{aligned} & 8A_{11}\pi r_0^4 + 5E_0A_1n_1r_1^3 + 5E_0A_1n_1r_0^3 + 8A_{11}r_1^4\pi \\ & \quad + 8r_0^3\pi A_{11}r_1 + \\ & + 8r_0^2\pi A_{11}r_1^2 + 8r_0\pi A_{11}r_1^3 + 5r_0^2E_0A_1n_1r_1 \\ & \quad + 5r_0E_0A_1n_1r_1^2 \end{aligned} \right) \\ & - \frac{3\pi\beta m^2}{4096(r_0-r_1)} \\ & \quad \left(\begin{aligned} & 8r_0^2\pi A_{11} - 40r_0^2\pi A_{12} + 3r_0E_0A_1n_1 + 8r_0\pi A_{11}r_1 \\ & -40r_0\pi A_{12}r_1 + 3E_{0*}A_1n_1r_1 + 8A_{11}\pi r_1^2 - 40r_1^2\pi A_{12} \end{aligned} \right) \\ & \quad + \frac{n^2(r_1^2+r_0r_1+r_0^2)(3A_{12}-2A_{66})\pi^4m^2}{192\beta(r_0-r_1)} \end{aligned} \right);$$

$$\begin{aligned} a_{310} = {} & \frac{\beta(r_0-r_1)\left((-1)^n-1\right)\left(r_0^4-r_1^4(-1)^m\right)}{\pi^2mn} \\ & - \frac{12\beta(r_0-r_1)^3\left((-1)^n-1\right)\left(r_0^2-r_1^2(-1)^m\right)}{\pi^4m^3n} \\ & + \frac{24\beta(r_0-r_1)^5\left((-1)^n-1\right)\left((-1)^m-1\right)}{n^2\pi^6m^5}. \end{aligned}$$

Appendix B

$$\begin{aligned} t_{11} = {} & \frac{(r_0-r_1)(r_0+r_1)}{8}\left(\frac{n^2A_{66}\pi^2}{\beta} - \frac{(A_{11}-2A_{22})\beta}{2} + \frac{\beta E_0A_2}{s_2}\right) \\ & + \frac{\pi\beta n_1E_0(r_0^2+r_0r_1+r_1^2)m^2A_1}{24(r_0-r_1)} + \frac{\pi^2\beta(r_0+r_1)(r_0^2+r_1^2)m^2A_{11}}{16(r_0-r_1)}; \end{aligned}$$

$$\begin{aligned} t_{12} = {} & -\frac{\pi^2mn^2(r_0^2+r_0r_1+r_1^2)(A_{66}+A_{12})}{12} \\ & + \frac{(r_0-r_1)^2(2A_{66}+A_{12}+A_{22})n^2}{8m} + \frac{E_0A_2(r_0-r_1)^2n}{8ms_2} \end{aligned}$$

$$t_{13} = t_{14} = 0;$$

$$\begin{aligned} t_{21} = {} & \frac{E_0A_2(r_0-r_1)^2n}{8ms_2} - \frac{\pi^2(r_0^2+r_0r_1+r_1^2)(A_{66}+A_{12})mn}{12} \\ & - \frac{(r_0-r_1)^2(-A_{22}+A_{12})n}{m}; \end{aligned}$$

$$\begin{aligned} t_{22} = {} & \frac{n^2(r_0^2-r_1^2)\pi^2}{8\beta}\left(A_{22} + \frac{E_0A_2}{s_2}\right) + \frac{A_{66}\beta\pi^2(r_0+r_1)(r_0^2+r_1^2)m^2}{16(r_0-r_1)} \\ & + \frac{3(r_0^2-r_1^2)A_{66}\beta}{16}; \end{aligned}$$

$$t_{23} = \frac{\pi B_{66}m\beta}{4};\ t_{24} = t_{31} = t_{32} = 0;$$

$$\begin{aligned} t_{33}: = {} & \left(\frac{m^2(r_0^2+r_0r_1+r_1^2)\pi^4n^2}{6\beta(r_0-r_1)} - \frac{n^2(r_0-r_1)\pi^2}{\beta}\right)D_{12} \\ & + \left(-\frac{(r_0-r_1)(r_0^2+r_0r_1+r_1^2)\pi^2n^2}{6R\beta} + \frac{(r_0-r_1)^3n^2}{4R\beta m^2}\right)B_{22} \\ & + \frac{\pi^4\beta m^4\left(r_0^4+r_0^2r_1^2+r_0r_1^3+r_0^3r_1+r_1^4\right)D_{11}}{20(r_0-r_1)^3} \\ & + \left(\frac{m^2(r_0^2+r_0r_1+r_1^2)\pi^2E_0\beta}{12(r_0-r_1)s_2} + \frac{n^2(r_0-r_1)\pi^2E_0}{2\beta s_2}\left(\frac{n^2\pi^2}{2\beta^2}-1\right) - \frac{(r_0-r_1)E_0\beta}{4s_2}\right)I_2 \\ & + \left(\frac{m^2(r_0+r_1)\beta n_1E_0\pi}{32(r_0-r_1)} + \frac{5\pi^3\beta E_0n_1(r_0r_1^2+r_0^2r_1+r_1^3+r_0^3)m^4}{160(r_0-r_1)^3}\right)I_1 \\ & + \left(-\frac{(r_0-r_1)(r_0^2+r_0r_1+r_1^2)\pi^2n^2}{6R\beta} + \frac{(r_0-r_1)^3n^2}{4R\beta m^2}\right)C_2 \\ & + \left(\begin{aligned} & \frac{(r_0-r_1)\left(r_0^4+r_0^2r_1^2+r_0r_1^3+r_0^3r_1+r_1^4\right)E_0\beta}{20R^2s_2} \\ & -\frac{(r_0^2+r_0r_1+r_1^2)(r_0-r_1)^3E_0\beta}{4\pi^2m^2R^2s_2} + \frac{3(r_0-r_1)^5\beta E_0}{8m^4R^2\pi^4s_2} \end{aligned}\right)A_2 \\ & + \left(\begin{aligned} & \frac{(r_0-r_1)\left(r_0^4+r_0^2r_1^2+r_0r_1^3+r_0^3r_1+r_1^4\right)\beta}{20R^2} \\ & -\frac{(r_0^2+r_0r_1+r_1^2)(r_0-r_1)^3\beta}{4\pi^2m^2R^2} + + \frac{3(r_0-r_1)^5\beta}{8m^4R^2\pi^4} \end{aligned}\right)A_{22} \\ & + \left(\begin{aligned} & \frac{(r_0-r_1)\left(r_0^4+r_0^2r_1^2+r_0r_1^3+r_0^3r_1+r_1^4\right)\beta}{20R^2} \\ & -\frac{(r_0^2+r_0r_1+r_1^2)(r_0-r_1)^3\beta}{4\pi^2m^2R^2} + + \frac{3(r_0-r_1)^5\beta}{8m^4R^2\pi^4} \end{aligned}\right)A_{11} \\ & + \left(\begin{aligned} & -\frac{(r_0^2+r_0r_1+r_1^2)(r_0-r_1)^3\beta}{2\pi^2m^2R^2} + \frac{3(r_0-r_1)^5\beta}{4m^4R^2\pi^4} \\ & + \frac{(r_0-r_1)\left(r_0^4+r_0^2r_1^2+r_0r_1^3+r_0^3r_1+r_1^4\right)\beta}{10R^2} \end{aligned}\right)A_{12} \\ & + \left(\begin{aligned} & \frac{(r_0-r_1)(r_0^2+r_0r_1+r_1^2)\beta}{4R} - \frac{3(r_0-r_1)^3\beta}{8RPi^2m^2} \\ & -\frac{m^2\left(r_0^4+r_0^2r_1^2+r_0r_1^3+r_0^3r_1+r_1^4\right)\beta\pi^2}{10(r_0-r_1)R} \end{aligned}\right)B_{11} \\ & + \left(\begin{aligned} & \frac{(r_0-r_1)(r_0+r_1)(r_0^2+r_0r_1+r_1^2)E_0n_1\beta}{32\pi R^2} \\ & -\frac{3(r_0-r_1)^3E_0n_1(r_0+r_1)\beta}{32\pi^3m^2R^2} - \frac{m^2(r_0+r_1)(r_0^2+r_1^2)\beta n_1z_1E_0\pi}{16(r_0-r_1)R} \end{aligned}\right)A_1 \\ & + \left(\begin{aligned} & \frac{n^4(r_0-r_1)\pi^4}{4\beta^3} + \frac{m^2(r_0^2+r_0r_1+r_1^2)\beta\pi^2}{12(r_0-r_1)} \\ & -\frac{n^2(r0-r1)\pi^2}{2\beta} - \frac{\beta(r_0-r_1)}{4} \end{aligned}\right)D_{22} + \left(\begin{aligned} & \frac{m^2(r_0^2+r_0r_1+r_1^2)\pi^4n^2}{3\beta(r_0-r_1)} \\ & -\frac{n^2(r_0-r_1)\pi^2}{2\beta} \end{aligned}\right)D_{66} \\ & + \left(\begin{aligned} & -\frac{(r_0-r_1)(r_0^2+r_0r_1+r_1^2)\pi^2n^2}{6R\beta} + \frac{(r_0-r_1)^3n^2}{4R\beta m^2} - \frac{3(r_0-r_1)^3\beta}{8R\pi^2m^2} \\ & -\frac{m^2\left(r_0^4+r_0^2r_1^2+r_0r_1^3+r_0^3r_1+r_1^4\right)\beta\pi^2}{10(r_0-r_1)R} + \frac{(r_0-r_1)(r_0^2+r_0r_1+r_1^2)\beta}{4R} \end{aligned}\right)B_{12} \end{aligned}$$

$$t_{34} = t_{35} = 0;$$

$$t_{36} = -\frac{(r_0^2+r_0r_1+r_1^2)(r_0-r_1)^3\beta}{4\beta^2m^2} + \frac{(r_0-r_1)\left(r_0^4+r_0^2r_1^2+r_0r_1^3+r_0^3r_1+r_1^4\right)\beta}{20} + \frac{3(r_0-r_1)^5\beta}{8m^4\pi^4};$$

$$t_{37} = \frac{(r0 - r1)^3}{8m^2}\left(\frac{3\beta}{2\pi^2} - \frac{n^2}{\beta}\right) + (r_0 - r_1)(r_0^2 + r_0 r_1 + r_1^2)\left(\frac{R\pi^2 n^2}{12R\beta} - \frac{\beta}{8}\right) + \frac{m^2\left(r_0^4 + r_0^2 r_1^2 + r_0 r_1^3 + r_0^3 r_1 + r_1^4\right)\beta\pi^2}{20(r_0 - r_1)};$$

$$t_{310} = \frac{\beta(r_0 - r_1)\left((-1)^n - 1\right)\left(r_0^4 - r_1^4(-1)^m\right)}{\pi^2 mn} - \frac{12\beta(r_0 - r_1)^3\left((-1)^n - 1\right)\left(r_0^2 - r_1^2(-1)^m\right)}{\pi^4 m^3 n} + \frac{24\beta(r_0 - r_1)^5\left((-1)^n - 1\right)\left((-1)^m - 1\right)}{n^2\pi^6 m^5}.$$

References

[1] G. Meiwen, E.H. Issam, Stability of eccentrically stiffened plates, Thin-Walled Struct. 14 (1) (1992) 1–20.
[2] N.D. Duc, P.H. Cong, Nonlinear postbuckling of an eccentrically stiffened thin FGM plate resting on elastic foundations in thermal environments, Thin-Walled Struct. 75 (2014) 103–112.
[3] N.E. Shanmugam, Y.S. Choo, M. Arockiaswamy, Experimental studies on stiffened plates under in-plane load and lateral pressure, Thin-Walled Struct. 80 (2014) 22–31.
[4] X.Q. Zhou, D.Y. Yu, X. Shao, S. Wang, Y.H. Tian, Band gap characteristics of periodically stiffened-thin-plate based on center-finite-difference-method, Thin-Walled Struct. 82 (2014) 115–123.
[5] Z.M. Li, P. Qiao, Nonlinear vibration analysis of geo-desically-stiffened laminated composite cylindrical shells in an elastic medium, Compos. Struct. 111 (2014) 473–487.
[6] S. Sarmila, Laminated composite stiffened shallow spherical panels with cutouts under free vibration – a finite element approach, Eng. Sci. Technol. Int. J. (2014) 1–13.
[7] D. Li, G. Qing, Y. Liu, A layerwise/solid-element method for the composite stiffened laminated cylindrical shell structures, Compos. Struct. 98 (2013) 215–227.
[8] Z.M. Li, D.Q. Yang, Post-buckling of shear deformable stiffened anisotropic laminated cylindrical shell under axial compression, Ocean Eng. 38 (2011) 1246–1255.
[9] J.B. Casimir, M.A. Khadimallah, M.C. Nguyen, Formulation of the dynamic stiffness of a crossply laminated circular cylindrical shell subjected to distributed loads, Comput. Struct. 166 (2016) 42–50.
[10] H. Less, H. Abramovich, Dynamic buckling of a laminated composite stringer stiffened cylindrical panel, Compos. Part B: Eng. 43 (5) (2012) 2348–2358.
[11] D.H. Bich, D.V. Dung, V.D. Long, Dynamic buckling of imperfect reinforced laminated composite plates and shallow shells, in: Proceedings of the International Conference on Computational Solid Mechanics, Hochiminh City, Vietnam, 2008, pp. 15–25.
[12] N.D. Duc, Nonlinear thermal dynamic analysis of eccentrically stiffened S-FGM circular cylindrical shells surrounded on elastic foundations using the Reddy's third-order shear deformation shell theory, Eur. J. Mech. – A/Solids 58 (2016) 10–30.
[13] N.D. Duc, N.D. Tuan, T.Q. Quan, N.V. Quyen, T.V. Anh, Nonlinear mechanical, thermal and thermo mechanical postbuckling of imperfect eccentrically stiffened thin FGM cylindrical panels on elastic foundations, Thin-Walled Struct. 96 (2015) 155–168.
[14] N.D. Duc, Nonlinear dynamic response of imperfect eccentrically stiffened FGM double curved shallow shells on elastic foundation, J. Compos. Struct. 99 (2013) 88–96.
[15] N.D. Duc, T.Q. Quan, Nonlinear post-buckling of imperfect eccentrically stiffened P-FGM double curved thin shallow shells on elastic foundations in thermal environments, J. Compos. Struct. 106 (2013) 590–600.
[16] N.D. Duc, T.Q. Quan, Nonlinear dynamic analysis of imperfect FGM double curved thin shallow shells with temperature-dependent properties on elastic foundation, J. Vib. Control 21 (7) (2015) 1340–1362.
[17] N.D. Duc, T.Q. Quan, Nonlinear post-buckling of imperfect double curved thin FGM shallow shells on elastic foundations subjected to mechanical loads, J. Mech. Compos. Mater. 49 (2013) 493–506.
[18] N.D. Duc, T.P. Thang, Nonlinear buckling of imperfect eccentrically stiffened metal-ceramic-metal S-FGM thin circular cylindrical shells with temperature-dependent properties in thermal environments, Int. J. Mech. Sci. 81 (2014) 17–25.
[19] N.D. Duc, T.P. Thang, Nonlinear response of imperfect eccentrically stiffened ceramic-metal-ceramic FGM circular cylindrical shells surrounded on elastic foundations and subjected to axial compression, J. Compos. Struct. 110 (2014) 200–206.
[20] D.H. Bich, V.H. Nam, N.T. Phuong, Nonlinear post-buckling of eccentrically stiffened functionally graded plates and shallow shells, Vietnam J. Mech. 33 (3) (2011) 131–147.
[21] D.H. Bich, D.V. Dung, V.H. Nam, Nonlinear dynamic analysis of eccentrically stiffened functionally graded cylindrical panels, J. Compos. Struct. 94 (2012) 2465–2473.
[22] M.M. Najafizadeh, A. Hasani, P. Khazaeinejad, Mechanical stability of functionally graded stiffened cylindrical shells, Appl. Math. Model. 54 (2) (2009) 1151–1157.
[23] S. Jiabin, C.W. Lim, X. Xinsheng, H. Mao, Accurate buckling solutions of grid-stiffened functionally graded cylindrical shells under compressive and thermal loads, Compos. Part B: Eng. 89 (2016) 96–107.
[24] D.H. Bich, N.T. Phuong, Buckling analysis of functionally graded annular spherical shells and segments subjected to mechanical loads, VNU J. Math. – Phys. 29 (3) (2013) 14–31.
[25] V.T.T. Anh, D.H. Bich, N.D. Duc, Nonlinear buckling analysis of thin FGM annular spherical shells on elastic foundations under external pressure and thermal loads, Eur. J. Mech. – A/Solids 50 (2015) 28–38.
[26] V.T.T. Anh, N.D. Duc, The nonlinear stability of axisymmetric FGM annular spherical shells under thermo-mechanical load, Mech. Adv. Mater. Struct. (2016), http://dx.doi.org/10.1080/15376494.2015.1091528.
[27] V.T.T. Anh, D.H. Bich, N.D. Duc, Nonlinear stability of thin FGM annular spherical segment in thermal environment, Vietnam J. Mech. VAST 37 (4) (2015) 285–302.
[28] N.D. Duc, Nonlinear Static and Dynamic Stability of Functionally Graded Plates and Shells, Vietnam National University Press, Hanoi 2014, p. 724 (Monograph).